

Synthesis and characterization of mesoporous c-ZrO₂ microspheres consisting of peanut-like nano-grains

Hui Zhang^{a,*}, Zhentao An^b, Fan Li^c, Qing Tang^b, Kathy Lu^d, Wenchao Li^c

^a School of Science, Beijing Jiaotong University, Beijing 100044, PR China

^b Institute of Process Engineering, Chinese Academy of Sciences, Beijing 100080, PR China

^c Department of Physical Chemistry, University of Science and Technology Beijing, Beijing 100083, PR China

^d Materials Science and Engineering Department, Virginia Tech, Blacksburg, VA 24061, USA

Received 10 September 2007; received in revised form 8 October 2007; accepted 11 October 2007

Available online 22 October 2007

Abstract

Smooth and spherical ZrO₂ particles were successfully synthesized by a novel spray technique and calcination at 600–800 °C. The synthesized ZrO₂ microspheres were characterized by scanning electron microscopy (SEM), transmission electron microscopy (TEM), high-resolution transmission electron microscopy (HRTEM), and X-ray diffraction (XRD). It was found that the synthesized ZrO₂ microspheres, which were mainly existed as c-phase, possessed a homogeneously mesoporous microstructure consisting of peanut-like nano-grains around 8–13 nm in width diameter.

© 2007 Elsevier B.V. All rights reserved.

Keywords: Spray reaction synthesis; Mesoporous c-ZrO₂ microspheres; Peanut-like nano-grains; TEM/HRTEM characterizations

1. Introduction

Self-assembly of monodisperse spheres is an extremely promising method to fabricate photonic crystals in the visible and near-infrared wavelength ranges [1–4]. By this method, SiO₂ and polystyrene spheres are widely used to assemble opal-like photonic crystals because these two monodisperse spheres with a size distribution of less than 5% are easy to attain. However, the properties of the prepared photonic crystals from either SiO₂ or polystyrene microspheres are not impressive due to relatively low refractive indices of SiO₂ (~1.45) and polystyrene (~1.59). Up to date, only a few groups have achieved the synthesis and crystallization of monodisperse colloidal spheres made from materials with a higher refractive index, like TiO₂ [5]. These new opals exhibit photonic band structures different from those of conventional opals owing to their assembly materials higher refractive indices relative to that of SiO₂ and polystyrene. ZrO₂, with a lower absorption in the visible and near-infrared regions and a relatively high refractive index (2.13–2.20), is another excellent candidate for use to create opal photonic crys-

tals with a novel photonic band structure. Lerot [6], Cantfort [7], and Yan [8] have synthesized the monodispersed ZrO₂ spheres by the hydrolysis of zirconium alkoxides, which is the only available technique to obtain ZrO₂ spheres with a narrow size distribution today, and assembled them into ordered structures by natural sedimentation. However, the production cost is high because of the expensive zirconium alkoxide starting materials. In this work, we present a new spray approach for synthesizing ZrO₂ microspheres with the aim of exploring possible route to produce monodisperse ZrO₂ spheres, which will be used for the construction of high quality ZrO₂ opal photonic crystals via self-assembly. Besides this application, high pure, mesoporous, and spherical ZrO₂ particles are also useful in advanced ceramics production, catalyst support, controlled drug release, etc. [9–12].

2. Experimental

An aqueous solution of ZrOCl₂·8H₂O (purity grade of 91.5%) was prepared by mixing the metal salt with distilled water and filtered with a filter paper to remove the solid impurity. NH₃ gas (purity grade of 99.9%) from ammonia cylinder was used as received.

A novel reaction method was used to produce ZrO₂ spheres. Fig. 1 shows the schematic reaction diagram. An aqueous solution ($c = 0.49\text{--}1.34\text{ mol L}^{-1}$) of ZrOCl₂·8H₂O was first atomized in the aerosol generator. After turning on the vacuum device, the aerosols of zirconium salt solution were carried into

* Corresponding author. Tel.: +86 010 51683627; fax: +86 010 51688433.
E-mail address: zhanghui14305@sohu.com (H. Zhang).

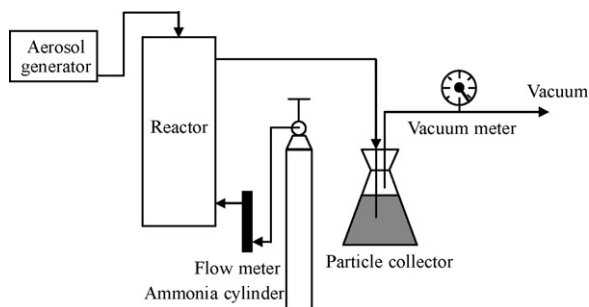


Fig. 1. A schematic diagram of the production system for ZrO_2 precursor spheres.

the reactor, into which NH_3 gas ($q_v = 8.33 \times 10^{-6} - 31.94 \times 10^{-6} \text{ m}^3 \text{ s}^{-1}$) from the cylinder with a pressure regulator was supplied. Thus, in the reactor quasi-gaseous phase reaction took place at room temperature between droplets of zirconium salt solution and NH_3 gas, which was also used as carrier gas in this method, forming the spherical ZrO_2 precursor (hydrated ZrO_2) particles. The produced ZrO_2 precursor spheres were carried into particle collector under a reduced pressure ($P = 92.50 - 100.37 \text{ kPa}$). The particle collector was filled with distilled water and used simultaneously as the buffering bottle. The collected ZrO_2 precursor spheres were washed several times with distilled water until no chloride ions could be detected in the supernatant solution. Afterwards, the cleaned ZrO_2 precursor spheres were washed twice with anhydrous ethanol to remove absorbed water molecules. Finally, the precursor spheres were dried in air at 80°C for 2 h and calcined in air at 350°C for 15 min, and at 600 , 700 , and 800°C for 2.5 h, respectively.

Sphere size and morphology were determined using HITACHI H-8100 TEM and Cambridge Stereoscan 250 MK 2 SEM. Average sphere sizes were estimated by counting 100 particles from representative TEM or SEM images of samples. The sphere microstructures were observed on a JEOL JEM2010 TEM. Specimens for TEM observation were prepared by embedding ZrO_2 precursor or ZrO_2 spheres in copper film by electrical chemical reaction, fixing the copper film wrapping spheres on the grid, and ion milling. Thermal analysis of ZrO_2 precursor powder was conducted on the thermal analyzer NETZSCH STA 449C to simultaneously obtain thermogravimetry and differential scanning calorimetry (TG/DSC). The phases in the powders were identified by Rigaku D/Max-2400 XRD using $\text{CuK}\alpha 1$ radiation.

3. Results and discussion

TEM (Fig. 2) and SEM (Fig. 3) images of ZrO_2 precursor spheres before and after drying clearly show fairly spherical

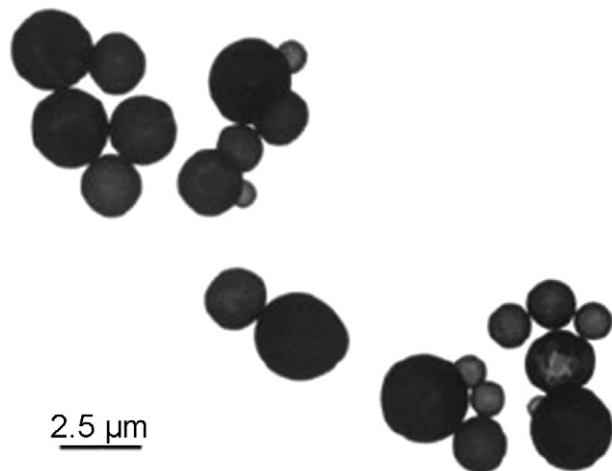


Fig. 2. TEM image of colloidal ZrO_2 precursor spheres.

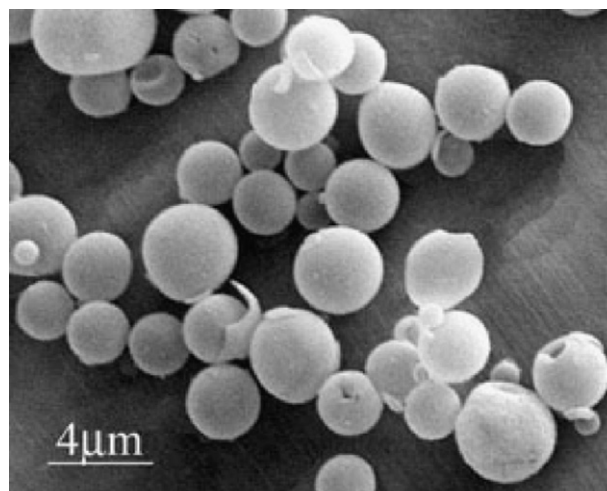


Fig. 3. SEM image of ZrO_2 precursor spheres after dried at 80°C for 2 h.

particles with a smooth surface. And SEM (Fig. 3) image of precursor spheres after drying illustrates an average size of $2.37 \mu\text{m}$ (relative standard deviation 0.22). These images demonstrated that the new technique could be successfully used to synthesize the ZrO_2 precursor spheres with a smooth surface, which was important for the construction of opal photonic crystal via self-assembly. However, some ZrO_2 precursor spheres were broken after drying. It is possible that these broken spheres were mostly formed from the larger aerosols that were mainly aggregates of smaller aerosols, and from those that were suspended in the upper section of the reactor. It can be reasonably proposed that during the precursor sphere formation, two steps could take place after the aerosols flew into the reactor. The first step was the dissolution of ammonia molecules in the zirconium salt solution droplets that acted as the microreactor. The second step was the precipitation of zirconium salt that occurred first at the surface of droplets. The speed of particle formation chiefly depended on the diffusion rates of the aqueous ammonia molecules and subsequently dissociated hydroxide ions at the droplet surface and the rate of precipitation. The reaction rate of precipitation should be much greater than that of diffusion because ZrO_2 pre-

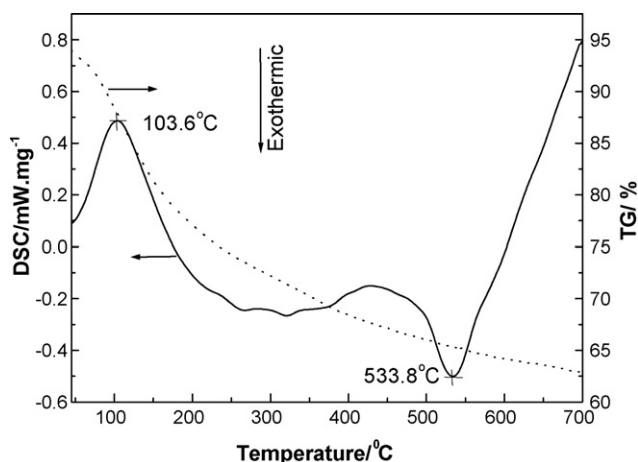


Fig. 4. TG/DSC curves of ZrO_2 precursor powder.

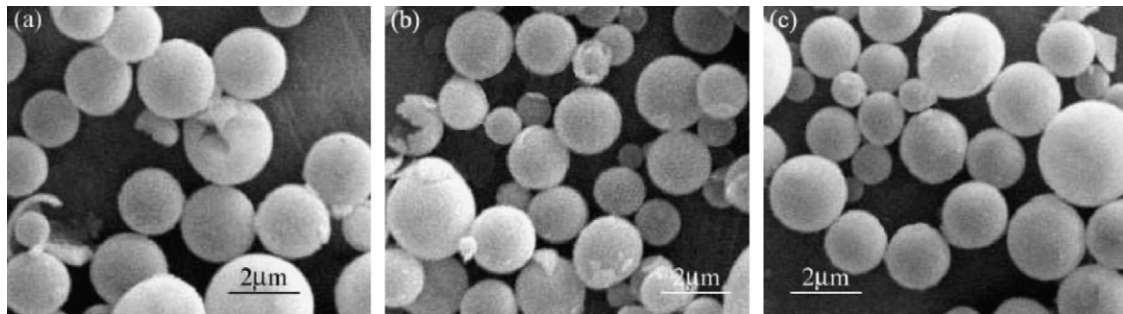


Fig. 5. SEM images of ZrO_2 microspheres after calcined at (a) 600 °C, (b) 700 °C, (c) 800 °C.

cursor ($\text{Zr}(\text{OH})_4$) produced at the surface of droplets prevented the diffusions of the aqueous ammonia molecules and hydroxide ions into the inside of droplets. Therefore, some of the larger aerosols and those floating in the upper section of the reactor were pumped into particle collector before they were reacted completely, resulting in the formation of spheres with a loose core and dense shell (hollow spheres). When these imperfect spheres were dried, the gas produced from the vaporization of a large amount of ethanol and residual water could not escape from the dense shells, resulting in sharp increase of the pressure inside the spheres and subsequent breaking of the spheres.

On the contrary, for those completely precipitated spheres with a homogeneous structure, the small amount of gas inside the spheres could be successfully released without damaging the spheres after drying. Moreover, Fig. 3 demonstrated that aggregations happened among spheres after drying. Aggregates were formed possibly due to hydrogen bonds between the hydroxyl groups of adjacent hydrous ZrO_2 spheres. After dehydration during drying, chemical bonds (Zr-O-Zr) between particles could be formed, resulting in hard aggregates [13]. Additionally, the residual chloride ions could also cause the formation of hard aggregates.

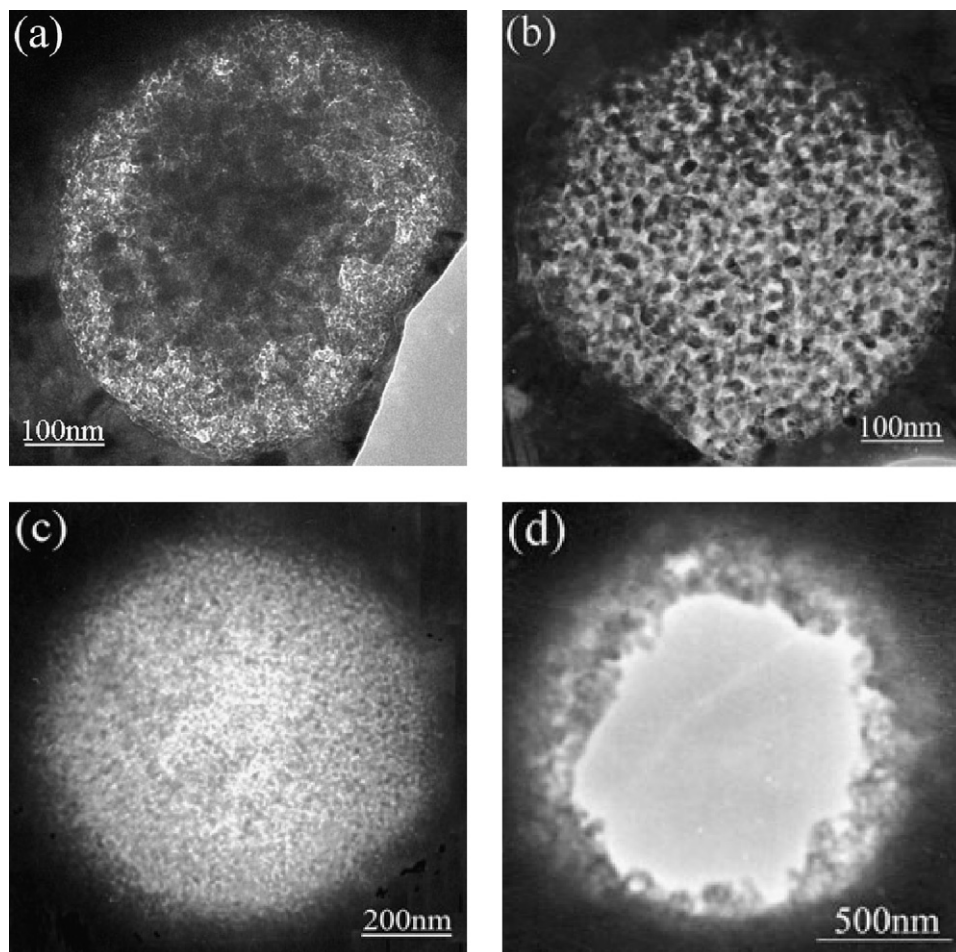


Fig. 6. Structures of the prepared ZrO_2 precursor (a) and ZrO_2 (b)–(d) microspheres. (a)–(b) the homogenous structure, (c) the structure with a loose core and dense shell, (d) the hollow structure.

Thermal analysis (Fig. 4) of ZrO_2 precursor particles illustrated their decomposition characteristics and phase transformation properties during heating (heating rate of 10.0 K/min). The DSC curve revealed an endothermic peak at around 103.6 °C, which corresponded to the volatilization and vaporization of the absorbed ethanol and water in the powder. The TG curve showed a significant weight loss of about 19.71% at around the corresponding peak temperature of 103.6 °C. Additionally, the DSC curve exhibited an exothermic peak at about 533.8 °C, which corresponded to the crystallization of ZrO_2 . It should be noted that the TG curve did not display a rapid weight loss at temperatures higher than 103.6 °C, nor the DSC curve presented any endothermic peak corresponding to structural dehydration. These data suggested that structural dehydration occurred almost through the whole heating process, even probably at around 103.6 °C.

SEM micrographs (Fig. 5) of ZrO_2 microspheres calcined at 600, 700, and 800 °C showed that the ZrO_2 particles after calcinations still kept the spherical shape and the sphere surface was smooth after crystallization. Average diameters of ZrO_2 microspheres calcined at different temperatures were 1.71 μm (600 °C, relative standard deviation 0.29), 1.63 μm (700 °C, relative standard deviation 0.34), and 1.66 μm (800 °C, relative standard deviation 0.30), respectively. In comparison with precursor spheres, ZrO_2 spheres calcined in the temperature range of 600–800 °C shrunk by 28–31% in size, stemming from the dehydration decomposition and the structural densification. Densification happened to those spheres with a porous structure. A detailed discussion about the shrinkage will be given later in this report.

As discussed, three kinds of structures of the precursor spheres were likely present, the homogenous, the soft core, and

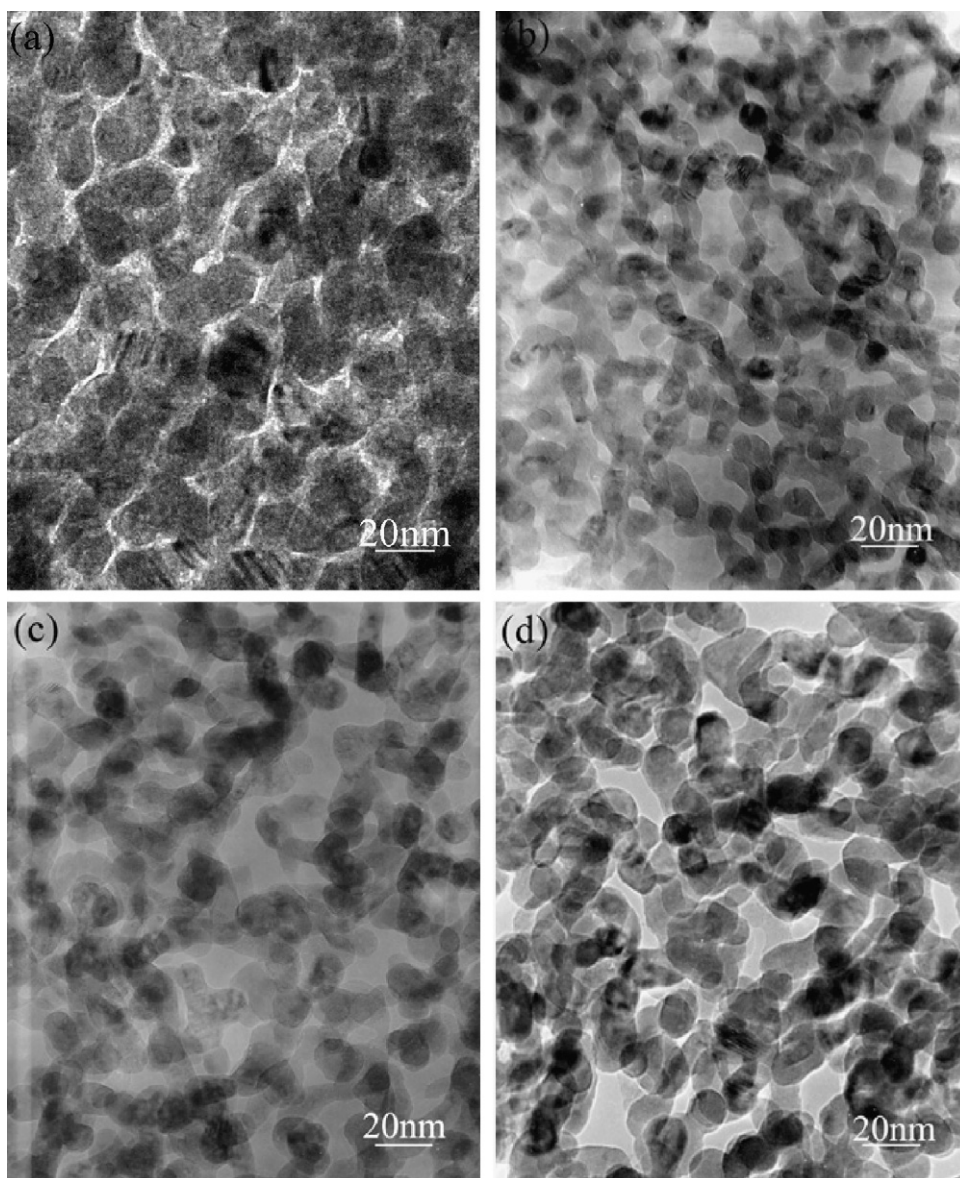


Fig. 7. Microstructures of the ZrO_2 spheres before (a) and after calcination at (b) 600 °C, (c) 700 °C, (d) 800 °C.

the hollow structures. Similar structures of ZrO_2 microspheres after calcinations were also found. Typical TEM micrographs (Fig. 6b–d) of cross sections of ZrO_2 microspheres obtained at 600–800 °C clearly demonstrated those three kinds of interior structures that ZrO_2 spheres possess, the homogeneous structure (Fig. 6b), the structure with a loose core and dense shell (Fig. 6c), and the hollow structure (Fig. 6d). The loose core and hollow structures were produced from those precursor spheres incompletely precipitated. As a comparison with Fig. 6b, we also presented a representative TEM image (Fig. 6a) of the cross section of a ZrO_2 precursor sphere with a homogeneous structure, where the central dark area was due to thick specimen. Fig. 6a,b revealed that those well-developed precursor and ZrO_2 spheres, formed from the completely precipitated precursor spheres, were a homogeneously porous structure. In order to further understand the interior microstructure and their formation of the well-developed ZrO_2 spheres before and after calcination at 600–800 °C, we conducted TEM/HRTEM examination of the cross sections of microspheres at high magnifications. The typical TEM micrographs (Fig. 7) of cross sections of spheres before and after calcinations at 600–800 °C evidently showed that both ZrO_2 precursor and heat-treated ZrO_2 microspheres were composed of peanut-like nano-particles/grains. The average width diameter (~16 nm) of nano-particles in precursor microspheres was larger than those (~8–13 nm) of nano-grains after heat treated at 600–800 °C. With the increase of calcination temperature, grain size grew from around 8 to 13 nm in width-diameter direction. Obviously, the pore size in precursor was smaller than those in heat-treated microspheres. This kind of mesoporous ZrO_2 microspheres is likely useful in advanced ceramics preparation, catalyst support, and controlled drug release.

XRD patterns (Fig. 8) of the spherical ZrO_2 precursor and ZrO_2 powders revealed the phase compositions in powders before and after calcination at 600–800 °C. It showed that ZrO_2 precursor spheres before calcination were amorphous, while all the ZrO_2 spheres calcined at 600–800 °C consisted of major c- ZrO_2 and minor t- ZrO_2 , and t- ZrO_2 content gradually rose with the increase of calcination temperature. It is known that the

stable phase for pure ZrO_2 is m- ZrO_2 below 1170 °C and subsequently t- ZrO_2 and c- ZrO_2 above 1170 °C. It is understandable that the precursor spheres were not crystalline phase before calcined, since not enough energy was provided for the precursor to dehydrate structurally and crystallize during synthesis at room temperature and drying at 80 °C for 2 h. An abnormal observation was that without doping with any bivalent or trivalent impurities, all the ZrO_2 microspheres calcined at 600–800 °C were not the stable monoclinic form, but mostly the phase at high temperature, c- ZrO_2 . This nonequilibrium behavior was also found in the published report [14], where pure ZrO_2 fine powders were produced by spray pyrolysis. It was most likely caused by the kinetics of the phase transformation process. It was shown from DSC curve that crystallization of ZrO_2 mainly took place at around 533.8 °C in this investigation. When the precursor was calcined at 600 °C, ZrO_2 generated by dehydration of the precursor gained kinetic energy high enough to crystallize. The transition from the highest-energy state to an intermediate energy state occurred with a much lower activation energy than the transition to the most stable state [15]. Another reason for the formation of c- ZrO_2 can be found in the structural relationships between the starting precursor and the final product. In general, high-temperature phases have a more open structure than low-temperature crystalline phases and consequently are more like the structure of a glassy precursor [15]. Additionally, the size of grains of nanometer scale in ZrO_2 microspheres is probably another reason for the metastable phases existing in lower temperature range. These factors tend to favor crystallization of c- ZrO_2 from amorphous precursor, even in the temperature range of stability of a lower temperature form. Therefore, a process of transformation from c- ZrO_2 to t- ZrO_2 to m- ZrO_2 can be expected with rising calcination temperature.

Figs. 9 and 10 are representative HRTEM images of cross sections of the precursor and heat-treated microspheres, respectively. It again demonstrated that the precursor was amorphous though some tiny crystalline particles were formed in the amorphous matrix, as indicated by arrowheads in Fig. 9. This

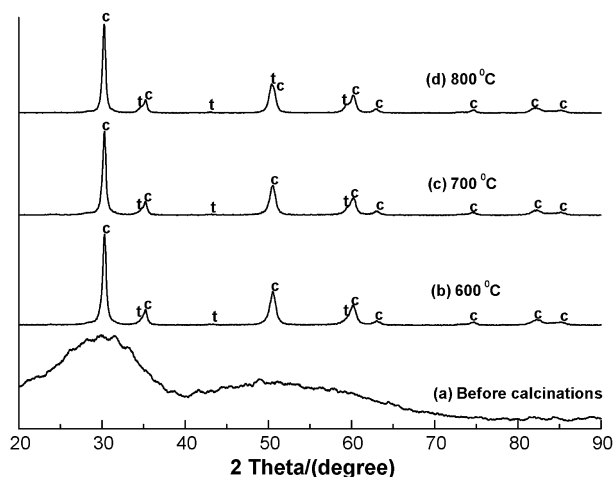


Fig. 8. XRD patterns of the spherical powders of ZrO_2 precursor (a) and ZrO_2 prepared at (b) 600 °C, (c) 700 °C, (d) 800 °C.

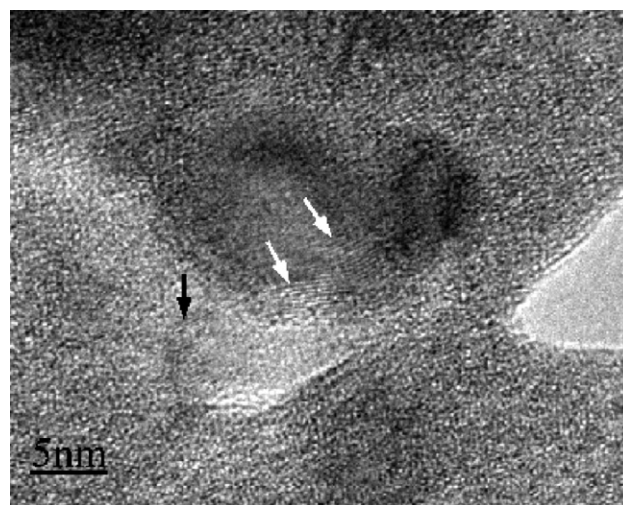


Fig. 9. A typical HRTEM picture of the cross section of the synthesized ZrO_2 precursor spheres.

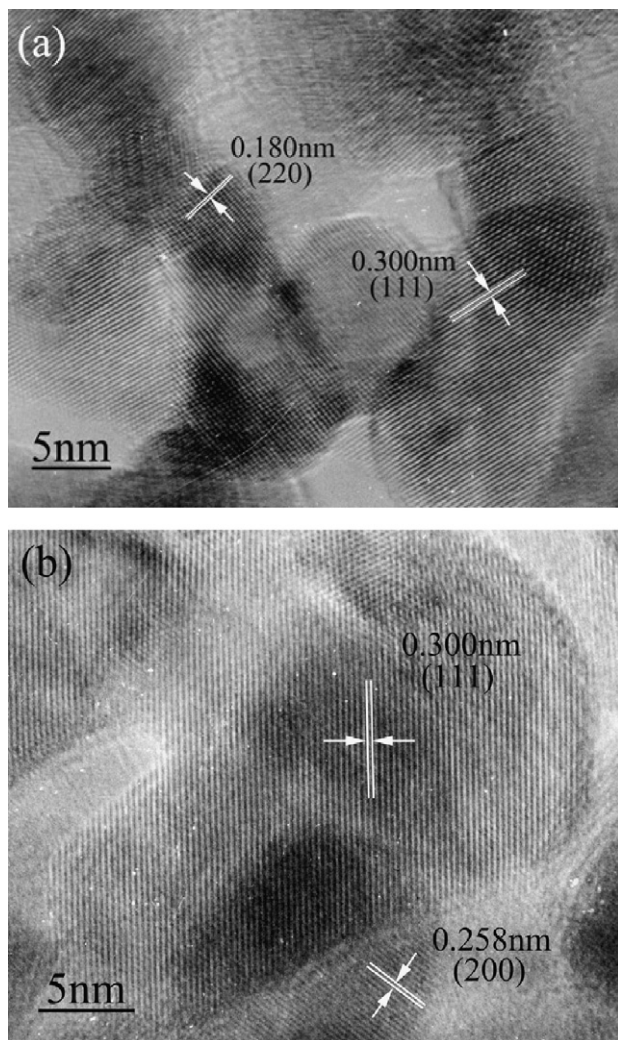


Fig. 10. Two typical HRTEM pictures of cross sections of the ZrO₂ microspheres obtained at 600–800 °C.

observation suggested that some crystals were formed during the preparation of precursor even though they cannot be detected by X-ray. Fig. 10 clearly showed the formation of c-ZrO₂ with (1 1 1), (2 2 0), and (2 0 0) planes in HRTEM pictures. However, t-phase was not found in all the HRTEM pictures taken. This was possibly because the spacings between crystalline planes of (1 1 1), (2 2 0), and (2 0 0) of t-phase were very close to the corresponding ones in c-phase. Therefore, they cannot be distinguished. Another reason was probably that t-ZrO₂ was so little that their lattice fringes cannot be photographed in our HRTEM images. Moreover, Fig. 10 showed more clear shapes and sizes of both peanut-like nano-grains and mesopores among grains.

We found that the size of ZrO₂ spheres decreased after calcination comparing with that before calcination. And the diameter of microspheres calcined at 700 °C continued to decrease comparing with that calcined at 600 °C. This size decrease indicated that the shrinkage in sizes of ZrO₂ microspheres prepared at 700 °C, resulting from the structural densification of ZrO₂ spheres during calcination, was bigger than the

enlargement in sizes, resulting from the increase of t-ZrO₂ content in microspheres (crystalline phase densities: c-ZrO₂ (6.27) > t-ZrO₂ (6.10) > m-ZrO₂ (5.68)). The size of microspheres produced at 800 °C was a little bigger than that of spheres calcined at 700 °C. This was because the size enlargement of microspheres produced at 800 °C, caused by further increase of the tetragonal phase content, was larger than the shrinkage caused by structural densification during calcination.

It should be pointed out that the colloidal ZrO₂ precursor spheres synthesized here were not monodisperse yet. Therefore, they cannot be used as building blocks to construct ordered photonic crystal structure. These problems will be further investigated and the synthetic process will be improved. However, mesoporous ZrO₂ spheres obtained here could still find other high-potential applications in advanced ceramics production, catalyst support, controlled drug release, chromatography separation, etc.

4. Conclusions

In summary, a novel spray technique for synthesizing ZrO₂ microspheres was developed. The prepared ZrO₂ spheres were characterized by SEM, TEM/HRTEM, and XRD. It was shown that fairly spherical ZrO₂ particles, with a smooth surface and an average diameter from 1.63 to 1.71 μm, were obtained by using the new process and calcination at 600–800 °C. The well-developed ZrO₂ microspheres had a homogeneously mesoporous microstructure with peanut-like nano-grains around 8–13 nm in width diameter. The phase compositions after calcination at 600–800 °C were mainly c-ZrO₂ with minor t-ZrO₂.

Acknowledgments

This work has been financed by both National Science Foundation of China (Grant No. 59974026) and Paper Foundation of Beijing Jiaotong University (Grant No. PD 282).

References

- [1] J.E.G.J. Wijnhoven, W.L. Vos, *Science* 281 (1998) 802.
- [2] P. Ni, P. Dong, B. Cheng, X. Li, D. Zhang, *Adv. Mater.* 13 (2001) 437.
- [3] S.H. Im, O.O. Park, *Langmuir* 18 (2002) 9642.
- [4] L. Xu, L.D. Tung, L. Spinu, A.A. Zakhidov, R.H. Baughman, J.B. Wiley, *Adv. Mater.* 15 (2003) 1562.
- [5] X. Jiang, T. Herricks, Y. Xia, *Adv. Mater.* 15 (2003) 1205.
- [6] L. Lerot, F. Legrand, P.D. Bruycker, *J. Mater. Sci.* 26 (1991) 2353.
- [7] O.V. Cantfort, B. Michaux, R. Pirard, J.P. Pirard, A.J. Lecloux, *J. Sol-Gel Sci. Techn.* 8 (1997) 207.
- [8] B. Yan, C.V. McNeff, F. Chen, P.W. Carr, A.V. McCormick, *J. Am. Ceram. Soc.* 84 (2001) 1721.
- [9] V. Belov, I. Belov, L. Harel, *J. Am. Ceram. Soc.* 80 (1997) 982.
- [10] P.M. Arnal, C. Weidenthaler, F. Schüth, *Chem. Mater.* 18 (2006) 2733.
- [11] A. Subramanian, P.W. Carr, C.V. McNeff, *J. Chromatogr. A* 890 (2000) 15.
- [12] J.B. Miller, E.I. Ko, *J. Catal.* 153 (1995) 194.
- [13] L. Jones, C.J. Norman, *J. Am. Ceram. Soc.* 71 (1988) C-190.
- [14] X. Dai, Q. Li, Y. Tang, *J. Am. Ceram. Soc.* 76 (1993) 760.
- [15] W.D. Kingery, H.K. Bowen, D.R. Uhlmann, *Introduction to Ceramics*, John Wiley & Sons, Inc., New York, 1975, p. 313.